Supplementary Information: Hogel-free Holography

PRANEETH CHAKRAVARTHULA, Princeton University and University of North Carolina at Chapel Hill
ETHAN TSENG, Princeton University
HENRY FUCHS, University of North Carolina at Chapel Hill
FELIX HEIDE, Princeton University

ACM Reference Format:
Praneeth Chakravarthula, Ethan Tseng, Henry Fuchs, and Felix Heide. 2022. Supplementary Information: Hogel-free Holography. *ACM Trans. Graph.* 1, 1 (July 2022), 11 pages. https://doi.org/10.1145/nnnnnnn.nnnnnnn

In this document we provide additional analysis and results in support of the primary text.

1 FURTHER ANALYSIS

Visualization of SLM phases. We showcase the SLM phase modulations generated by Holographic Stereogram (HS), Phase Add Stereogram (PAS), Overlap Add Stereogram (OLAS), and our proposed Hogel-Free Holography (HFH) in Fig. S1. As HFH does not rely on hogels and is not restricted by object phase constraints, the phase map can be finely catered to the target scene through optimization.

Optimization visualization. We present a visualization of our optimization process and how the quality of the 3D generated hologram improves in Fig. S2 and in the Supplementary Video.

Robustness to SLM phase non-linearities and image quality degradation. We compared the robustness of our method to SLM phase non-linearities against the previous state-of-the-art approach, Overlap Add Stereograms [2], in Sec. 6 of the main manuscript. We provide additional qualitative comparison in Fig. S3. As can be seen from the figure, hogel-free holograms are more robust to model mismatches and SLM deviations compared to OLAS and non-idealities result in only minor quality degradation. On the other hand, the quality of holographic reconstructions from the OLAS method deteriorate quite remarkably even with slight deviations.

SLM calibration and look-up tables. Our SLM does not support custom look-up table calibration due to its age. Although our method achieves a significant improvement in image quality in simulations, the experimental captures still suffer from residual aberrations arising from our prototype display. To further analyze the image quality from our experimental prototype, we measured the diffraction efficiency from a grating pattern with a period of 10 pixels, where odd numbered columns are fixed at a gray scale zero value and for even numbered columns the gray scale values were increased from 0 to 255 in steps of 4. If the SLM supports a full 2π-phase range and if the look-up tables which map voltages to phase modulation are calibrated correctly, then the light intensity

Authors' addresses: Praneeth Chakravarthula, cpk@cs.unc.edu, Princeton University and University of North Carolina at Chapel Hill, Chapel Hill, NC; Ethan Tseng, eftseng@cs.princeton.edu, Princeton University, Princeton, NJ; Henry Fuchs, fuchs@cs.unc.edu, University of North Carolina at Chapel Hill, Chapel Hill, NC; Felix Heide, fheide@cs.princeton.edu, Princeton University, Princeton, NJ.

Permission to make digital or hard copies of all or part of this work for personal or classroom use is granted without fee provided that copies are not made or distributed for profit or commercial advantage and that copies bear this notice and the full citation on the first page. Copyrights for components of this work owned by others than ACM must be honored. Abstracting with credit is permitted. To copy otherwise, or republish, to post on servers or to redistribute to lists, requires prior specific permission and/or a fee. Request permissions from permissions@acm.org.
© 2022 Association for Computing Machinery.
0730-0301/2022/7-ART $15.00
https://doi.org/10.1145/nnnnnnn.nnnnnnn

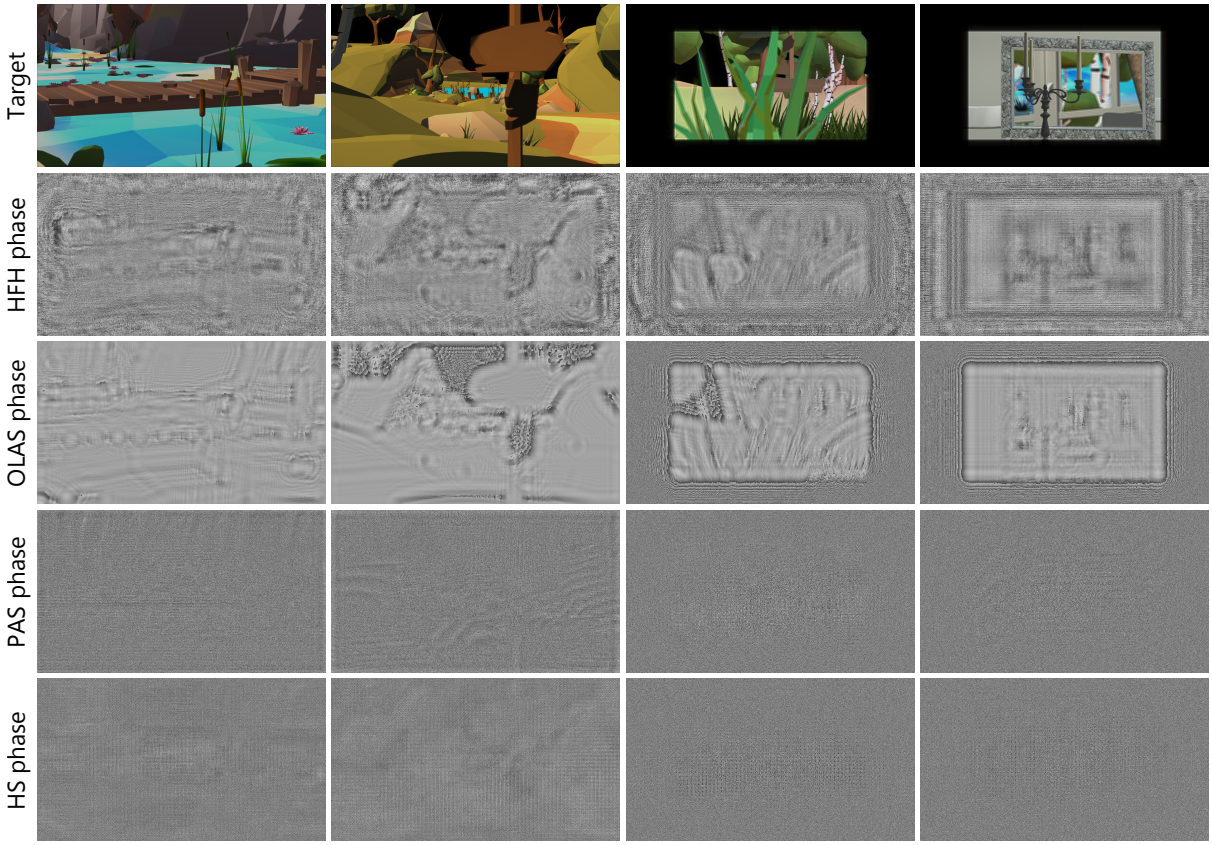

Fig. S1. *Visualization of holographic phase patterns.* We visualize the phase-only holograms for different existing holographic stereogram approaches and the proposed hogel-free holography method. HS and PAS spatially divide the entire hologram into sub-holograms or "hogels" thereby resulting in a spatio-angular resolution trade-off similar to that of light field displays. OLAS on the other hand computes several such hogels and overlaps them. HFH on the other hand does not compute hogels during optimization and as a result produces fine-tuned phase maps that generate the best 3D holograms compared to any existing methods.

in the central order will decrease until the phase difference between the odd and even columns is maximized (i.e. a phase difference of π). After decreasing, the light intensity will then proceed to increase due to the phase wrapping at 2π. This intensity plot is called the diffraction efficiency of the SLM.

To measure the diffraction efficiency of the SLM, we placed a Thorlabs S142C power meter at the Fourier plane of the SLM which is illuminated with a collimated laser beam. We show our setup in Fig. S4 and the measured diffraction efficiency in Fig. S5. However, as can be seen in Fig. S5, the diffraction efficiency curve of our SLM does not follow the expected trend and only supports a limited phase range with non-linear phase modulation. This resulted in the residual artifacts in our experimental results compared to simulations. Unfortunately, our SLM does not support custom look-up table calibration due to its age.

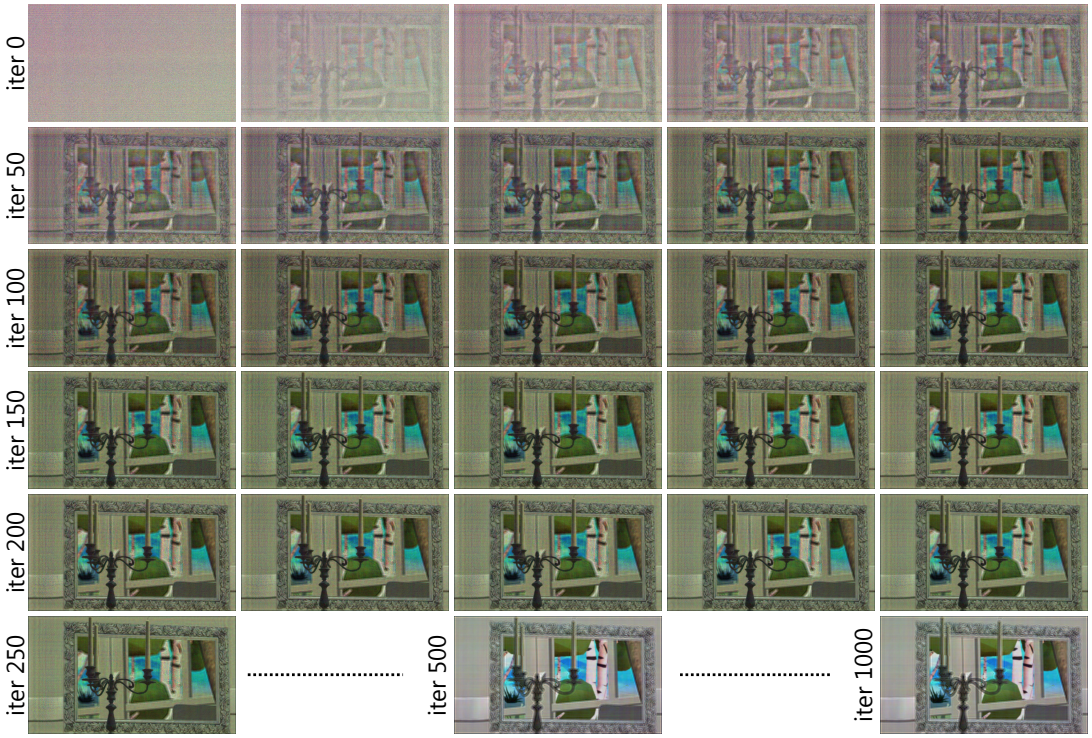

Fig. S2. *Optimization visualization.* Here we show how the 3D generated hologram improves during the optimization process.

2 FURTHER EXPERIMENTAL RESULTS

2.1 Stereograms versus Hogel-free Holograms

Existing light-field based holography methods rely on computing stereograms by spatially dividing the phase-only hologram into several sub-holograms or hogels, where each hogel encodes a specific angular view of the light field. While these are perhaps the only existing holography approaches promising true per-pixel focus as well as view-dependent effects, the stereogram approaches suffer from a fundamental spatio-angular resolution trade-off similar to light field displays. As a result, both high-quality reconstructions as well as diverse spatial/angular frequencies cannot be achieved simultaneously. The overlap-add stereogram method [2] attempts to fix this limitation by computing overlapping hogels, thereby increasing the spatial and angular resolution. However, all existing methods compute a complex wave field at the SLM and rely on heuristic encodings such as double phase amplitude coding [1]. This results in sub-optimal 3D holograms whose projections show severe artifacts and reduced light efficiency. Moreover, such approaches are not robust to phase non-linearities in the SLM as discussed in the main manuscript.

Hogel-Free Holography lifts this limitation for the first-time to the best of our knowledge and directly computes a true 3D phase-only hologram that shows both depth- and view-dependent effects. The hogel-free holograms do not compute explicit hogels corresponding to the light field as the other methods, thereby resulting in superior holographic reconstruction, completely overcoming the spatio-angular resolution trade-off. Furthermore, as we directly optimize for phase-only holograms, we do not require any heuristic encoding of complex wave fields on the SLM. This increases the image fidelity, contrast, and overall light efficiency/brightness of the holographic

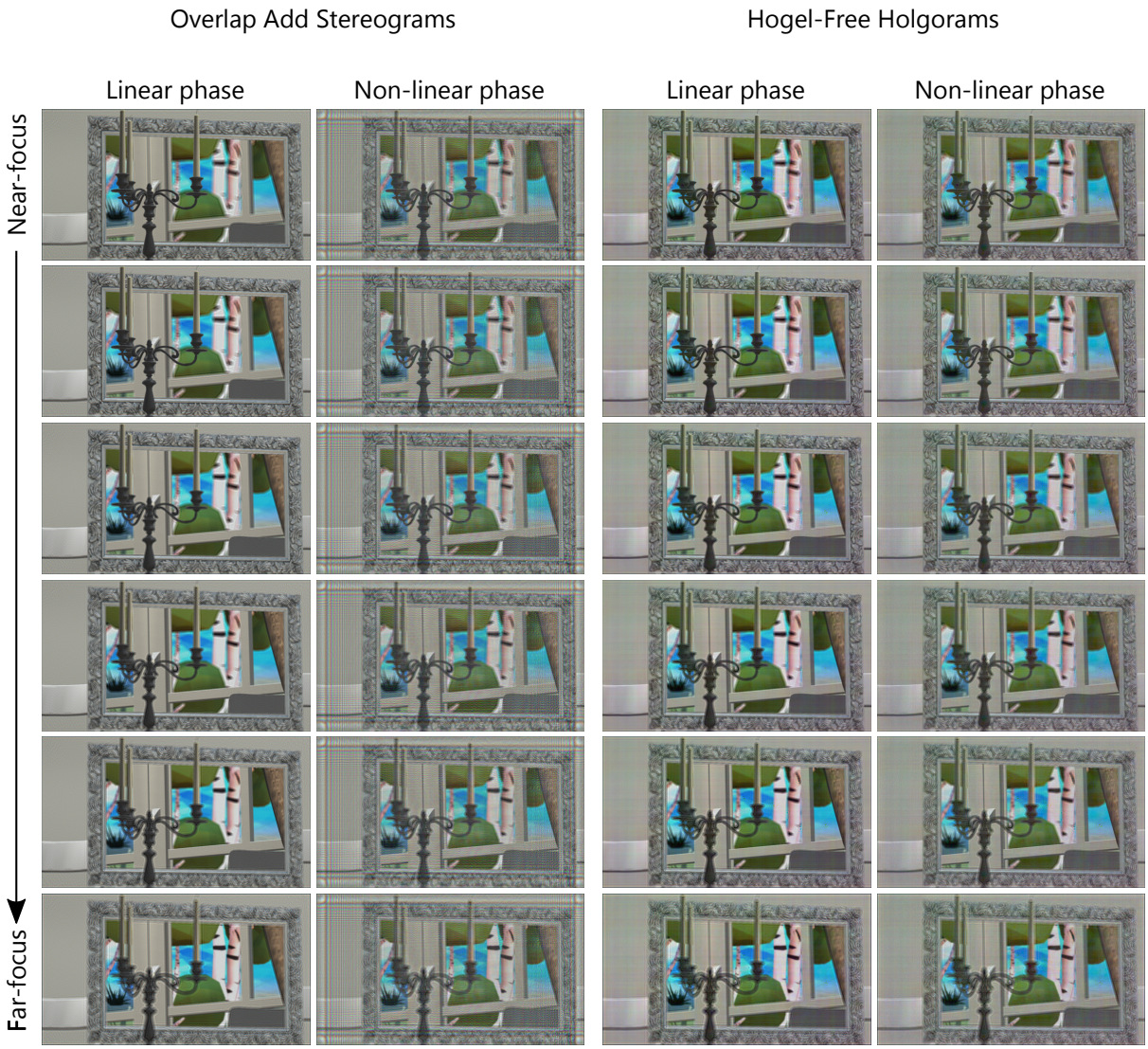

Fig. S3. *Robustness to phase non-linearities.* We visualize the simulated reconstructions of both OLAS and HFH holograms at uniformly sampled depths across the depth-of-the-field of the scene. As can be seen, OLAS provides reasonable reconstructions with a linear phase modulation on the SLM. However, even with slight non-linearity, the image quality degrades significantly. On the other hand, hogel-free holograms are more robust to phase non-linearities and SLM deviations, compared to the previous methods. Please zoom into the electronic version of this document for better viewing.

image. We also avoid the spatial resolution loss typical to double phase encoding caused by spatial sharing of SLM pixels for encoding both the amplitude and phase. Fig. S9 compares the hogel-free hologram phase with that of the OLAS phase.

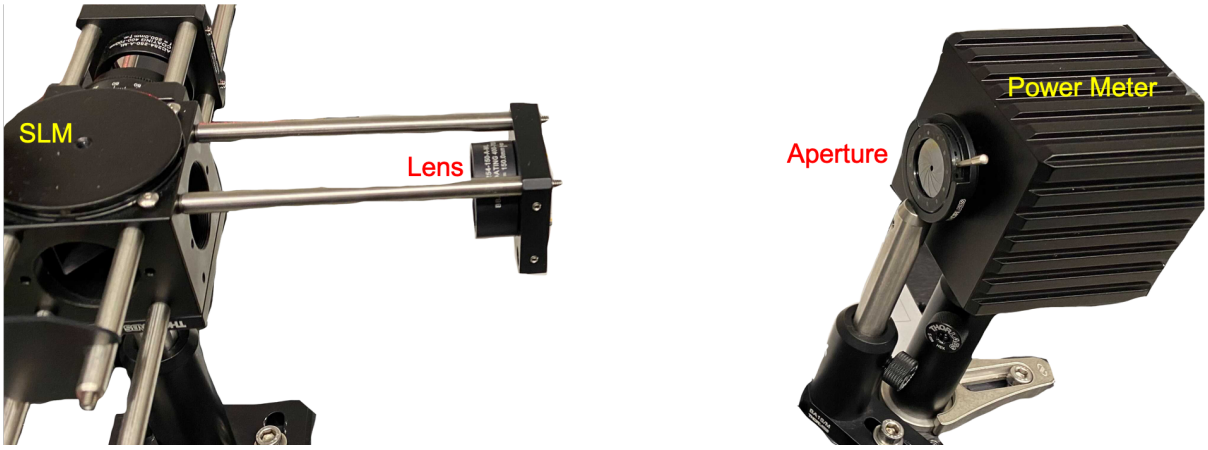

Fig. S4. *Setup for measuring SLM diffraction efficiency.* We place a Thorlabs S142C power meter at the Fourier plane of the SLM. The SLM is illuminated with a collimated laser beam and we filter the central order with an iris in order to measure the diffracted light efficiency.

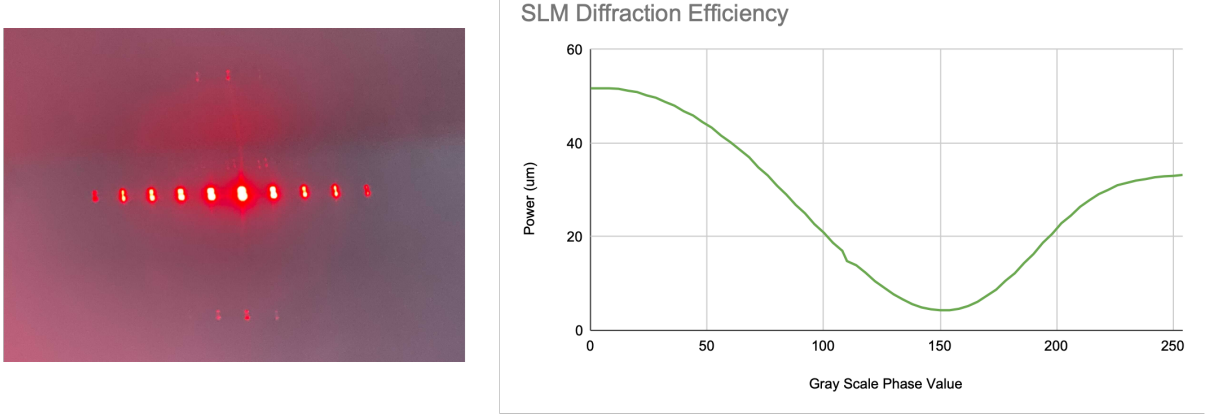

Fig. S5. *SLM diffraction efficiency.* We visualize the diffraction efficiency of the SLM. On the left, we show the diffracted intensity pattern on the Fourier plane of our input grating phase pattern on the SLM. We filter the central order with an iris before measuring the power. For a full 2π phase range the light intensity in the central order decreases and increases back up due to phase wrapping. However, as can be seen, our SLM supports a limited phase range with non-linear phase modulation which resulted in the residual artifacts in our experimental results compared to simulations. Our SLM does not support custom look-up table calibration due to its age.

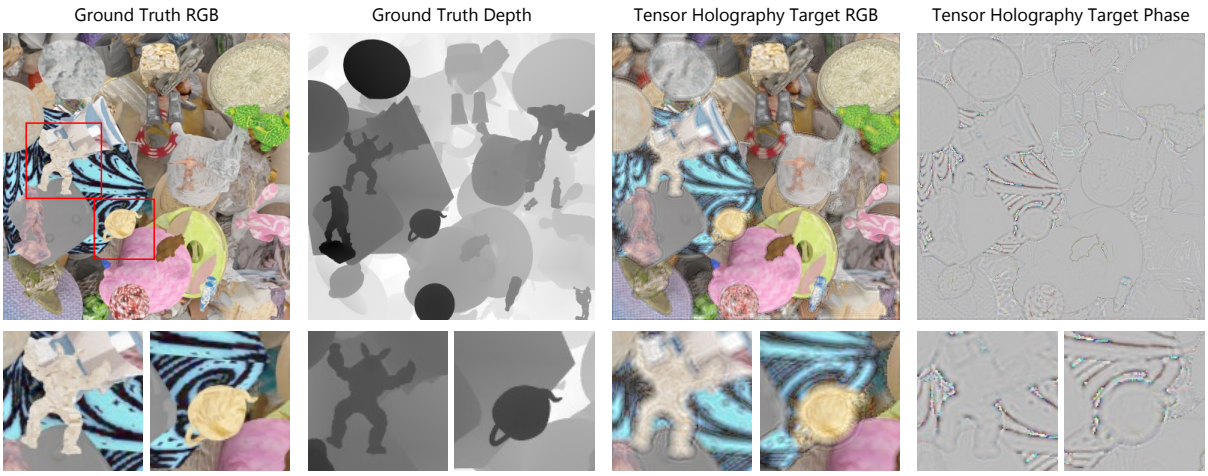

Fig. S6. *Inaccurate target in Tensor holography.* We visualize a randomly chosen plane from the target focal stack as well as the ground truth images used in Tensor holography [3]. The ground truth RGB (left) and corresponding depth images (middle left) features sharp edges. However, the target focal stack used as input to tensor holography (middle right) show artifacts at depth discontinuities which also manifest in the corresponding target phase patterns that use the ray-based visibility test (right).

2.2 Tensor holography compared to Hogel-free Holography Recently, Tensor holography [3] has been proposed as a method for displaying holograms of three-dimensional (3D) scenes with continuous depths cues. The core of this approach is a modified point-based hologram computation method. Typically, point-based methods do not model occlusion, preventing accurate recreation of complex 3D scenes where the foreground is severely contaminated by ringing artifacts due to the unoccluded background. Tensor holography tries to mitigate this problem by adding a per-ray visibility test. However, the quality of the resulting holograms is limited by the RGB-D representation employed in [3], which is fundamentally incomplete, and the ray-based visibility test, which does not accurately handle occlusions. We also show this in Fig. S6. As a result, tensor holography cannot model physically accurate occlusions and defocus cues.

We note that for RGB-D scene representations, only the front-most surfaces, that are directly visible to the user (or camera), is often fed as the input to hologram computation routines. As such, this approach does not consider occlusions and view-dependent effects. To consider some mutual occlusions, researchers have used ray casting methods in combination with point-based or polygonal-based methods such as in Shi et al. [3]. To better understand the impact of the input representaiton on reproducing occlusion-aware defocus, we show the target focal stack of images used by Tensor holography approach to compute holograms in Fig. S7. The occlusion edges are inaccurately represented with visible artifacts and depth discontinuities.

Hogel-Free Holography lifts this limitation and accurately represents both depth- and view-dependent effects by using RGB-D light fields as input. Note that light fields are nothing but a coerse sampling of continuous wave field. Therefore, as a result of optimizing for a target wave field, hogel-free holograms accurately represent also the underlying light field and hence accurate occlusions and defocus cues. This can be seen in the defocus

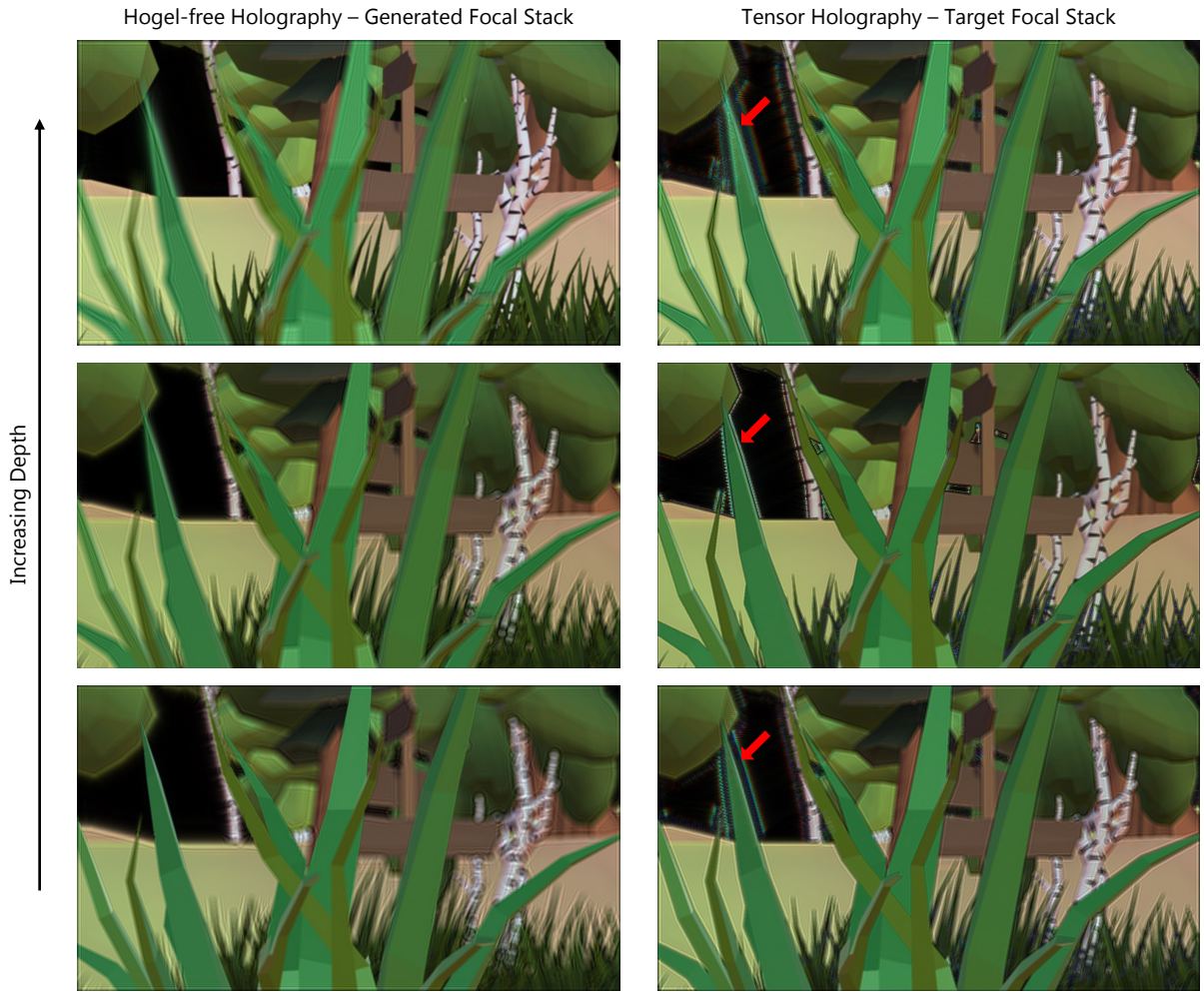

Fig. S7. *Target focal stacks for Hogel-free holography Tensor holography.* Here we visualize samples of the target focal stack used for Tensor holography and compare it against the focal stack generated by the wave representation of our input light field. As can be seen, our input wave representation exhibits accurate defocus near the grass blade (red arrows), wheras the defocus is not accurately modeled at the occlusion boundaries for Tensor holography. This discrepancy in the targets results in holograms with significant errors for Tensor holography.

cues represented by the focal stack of images by hogel-free holograms shown in Fig. S7. Compared to Tensor holography, a reduction in artifacts can be seen at the edges and depth discontinuities.

2.3 Experimental procedure

We compute the hogel-free holograms (HFH) using the end-to-end optimization technique described in the main manuscript. The optimization was implemented in PyTorch. All other holograms (*i.e.* Holographic Stereogram (HS), Phase Added Stereogram (PAS) and Overlap Add Stereogram (OLAS)) have been computed using the

code provided by the authors of the Overlap Add Stereogram method [2][1]. To image our true 3D holographic projections with different parts of the scene coming into and going out focus, we first display holograms computed for a calibration dot pattern and a Siemens star target at various distances. The camera is adjusted to focus on the calibration targets first. The captured calibration targets at arbitrarily sampled distances are shown in Fig. S8. This calibration procedure ensures that the captured scene is in sharp focus at the desired distance. As a reference, it can be seen that the high frequency regions in the Siemens star pattern are captured with high fidelity. Note that the holograms for the calibration patterns were also computed using our proposed HFH method. Additional experimental results are shown in Fig. S10, apart from those presented in the main manuscript.

[1]https://github.com/computational-imaging/olas

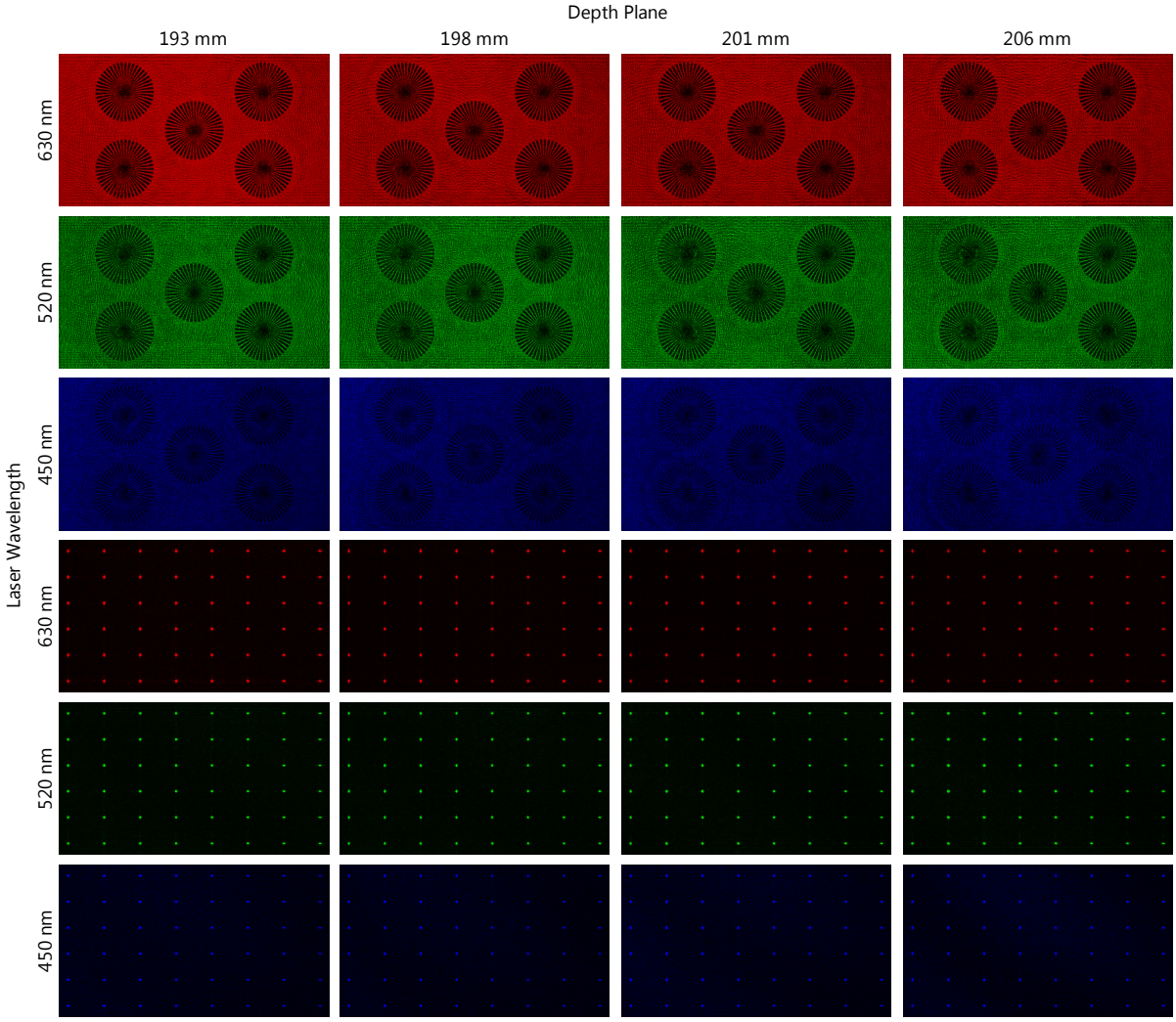

Fig. S8. *Calibration targets.* We used the Siemens Star pattern and the dot pattern to ensure that the camera is focused throughout the 3D volume being imaged. Note that the holograms for the calibration patterns were also computed using our proposed HFH method.

REFERENCES

[1] Andrew Maimone, Andreas Georgiou, and Joel S Kollin. 2017. Holographic near-eye displays for virtual and augmented reality. *ACM Transactions on Graphics (TOG)* 36, 4 (2017), 85.

[2] Nitish Padmanaban, Yifan Peng, and Gordon Wetzstein. 2019. Holographic near-eye displays based on overlap-add stereograms. *ACM Transactions on Graphics (TOG)* 38, 6 (2019), 214.

[3] Liang Shi, Beichen Li, Changil Kim, Petr Kellnhofer, and Wojciech Matusik. 2021. Towards real-time photorealistic 3D holography with deep neural networks. *Nature* 591, 7849 (2021), 234–239.

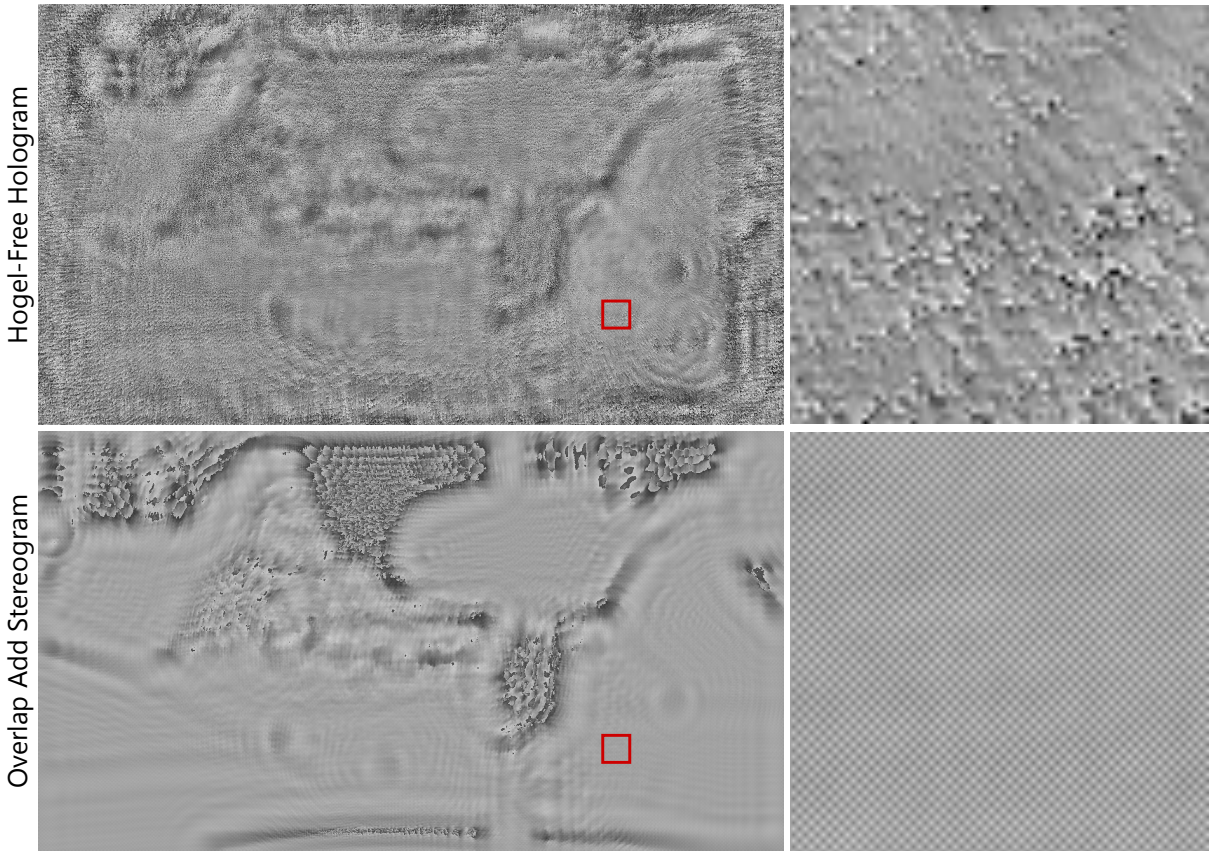

Fig. S9. *Comparison of HFH vs OLAS phase.* Here we compare the phase patterns of HFH and OLAS. OLAS heuristically encodes a complex wave field into a phase-only hologram by spatially sharing the SLM pixels. This encoding of a single complex value into two phase-only pixels results in a noticeable drop in spatial resolution. On the other hand, HFH directly optimizes for a phase-only hologram pattern, overcoming the limitations of all existing 3D hologram methods so far.

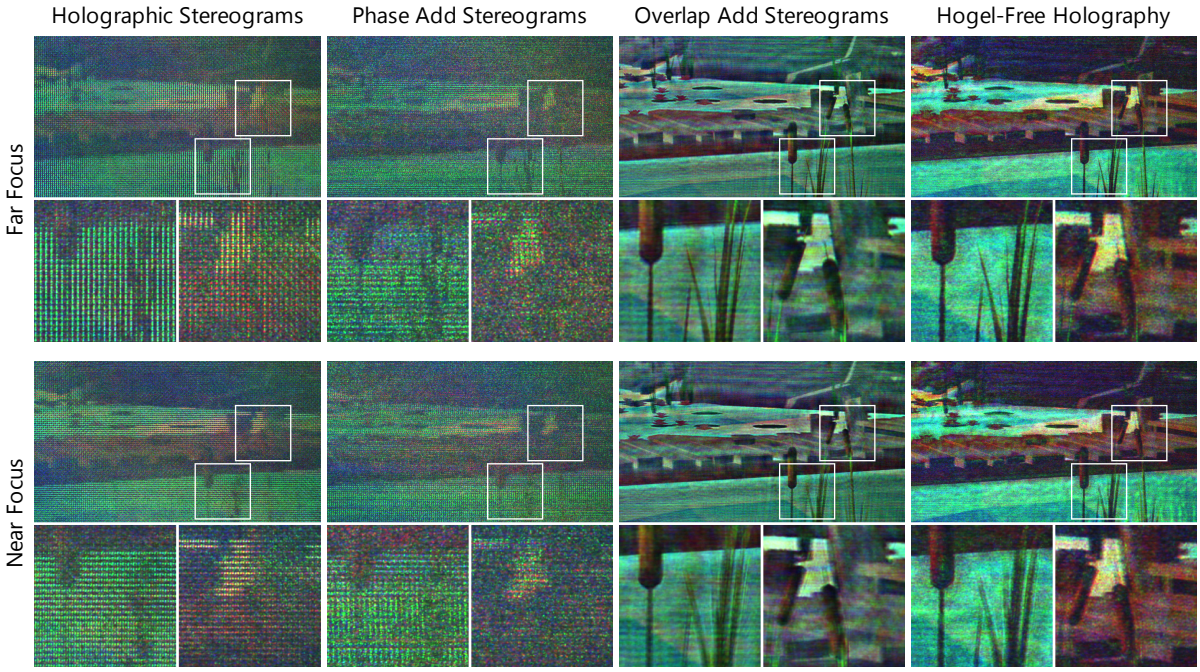

Fig. S10. *Additional experimental results.* Additional result using experimental prototype.